iScience

CellPress

Article

Surface LSP-1 Is a Phenotypic Marker Distinguishing Human Classical versus Monocyte-Derived Dendritic Cells

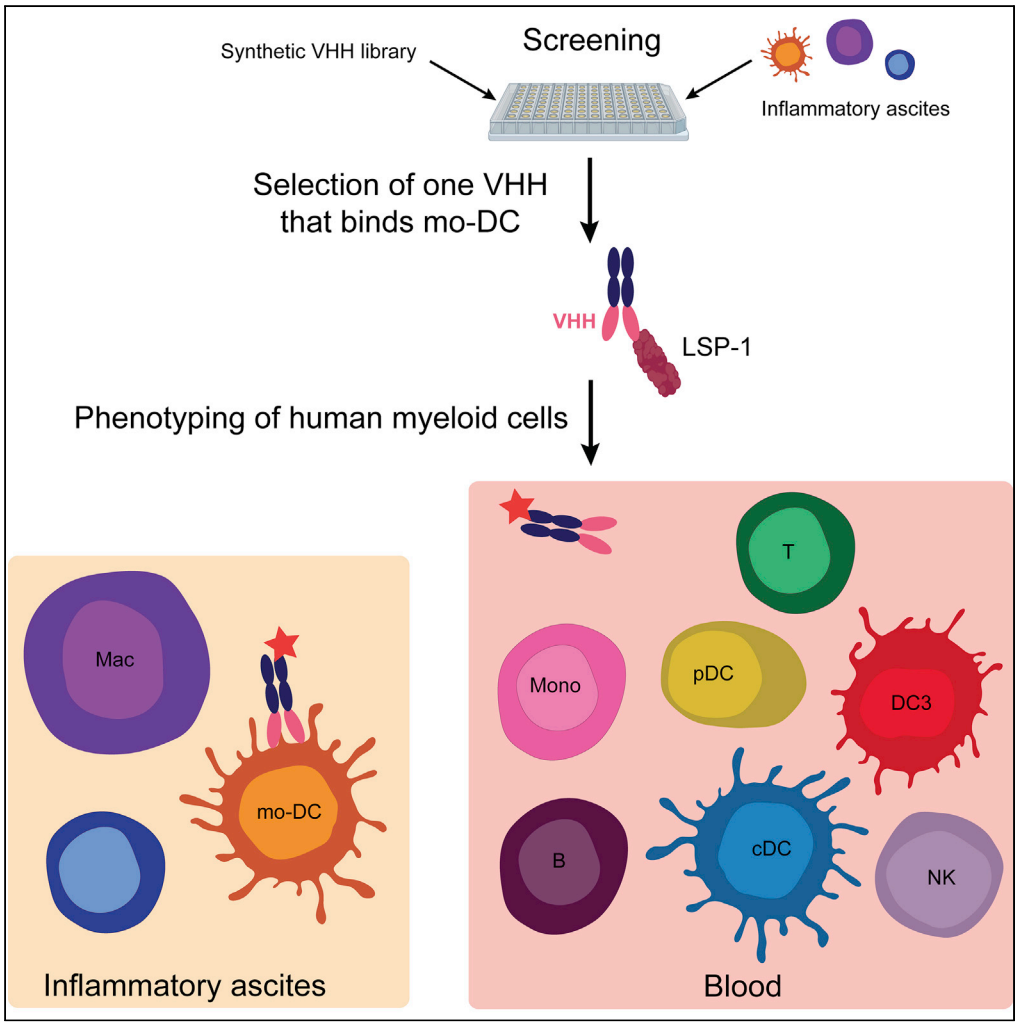

Sandrine Moutel, Anne Beugnet, Aurélie Schneider, ..., Sebastian Amigorena, Franck Perez, Elodie Segura

elodie.segura@curie.fr

HIGHLIGHTS

Identification of a humanized llama single chain antibody recognizing surface LSP-1

Surface LSP-1 is a specific marker of monocyte-derived dendritic cells

Classical dendritic cells or blood "DC3" are not stained by the antibody

Surface LSP-1 may be a useful marker for analyzing myeloid cells in human disease

DATA AND CODE AVAILABILITY

PXD015647

Moutel et al., iScience *23*, 100987
April 24, 2020
https://doi.org/10.1016/j.isci.2020.100987

iScience

CellPress

Article

Surface LSP-1 Is a Phenotypic Marker Distinguishing Human Classical versus Monocyte-Derived Dendritic Cells

Sandrine Moutel,[1] Anne Beugnet,[1] Aurélie Schneider,[1] Bérangère Lombard,[2] Damarys Loew,[2] Sebastian Amigorena,[3] Franck Perez,[1] and Elodie Segura[3,4,*]

SUMMARY

Human mononuclear phagocytes comprise several subsets of dendritic cells (DCs), monocytes, and macrophages. Distinguishing one population from another is challenging, especially in inflamed tissues, owing to the promiscuous expression of phenotypic markers. Using a synthetic library of humanized llama single domain antibodies, we identified a novel surface marker for human naturally occurring monocyte-derived DCs. Our antibody targets an extra-cellular domain of LSP-1, specifically on monocyte-derived DCs, but not on other leukocytes, in particular monocytes, macrophages, classical DCs, or the recently described blood DC3 population. Our findings will pave the way for a better characterization of human mononuclear phagocytes in pathological settings.

INTRODUCTION

Mononuclear phagocytes play a central role in the initiation and resolution of innate and adaptive immune responses. They comprise several populations of monocytes, macrophages, and dendritic cells (DCs), which are classically defined by their phenotype and ontogeny (Guilliams et al., 2014). Monocytes are very plastic cells and can differentiate into cells displaying typical features of macrophages or DCs, referred to as monocyte-derived macrophages (mo-Mac) and monocyte-derived DCs (mo-DC). This phenomenon has been described *in vitro* and *in vivo*, in both mouse and human (Jakubzick et al., 2017; Coillard and Segura, 2019; Ginhoux and Guilliams, 2016). Recently, high-resolution single-cell technologies have revealed a new subset of blood DCs, termed DC3, displaying a mixed transcriptomic profile of classical DC (cDC) and monocyte genes (Bakdash et al., 2016; Dutertre et al., 2019; Villani et al., 2017), reminiscent of that of mo-DC (Segura et al., 2013; Goudot et al., 2017). Whether blood DC3 represent circulating mo-DC has been unclear.

Accumulating evidence suggests that monocyte-derived cells are involved in the pathogenesis of autoimmune and chronic inflammatory diseases (Coillard and Segura, 2019). However, their characterization in inflamed tissues is complicated by the promiscuous expression of numerous phenotypic markers, shared in particular with macrophages and cDCs. More specific markers are needed in order to advance our understanding of the respective properties of macrophages, cDCs, and mo-DC, and ultimately to allow the manipulation of these cells for therapeutic strategies.

To identify novel markers for human mo-DC, we have used a synthetic library of humanized llama single domain antibodies. We identified one antibody, recognizing surface LSP-1, that stains specifically mo-DC, but not monocytes, macrophages, cDCs, or DC3.

RESULTS

In order to identify novel surface markers for human naturally occurring mo-DC, we set up a phage display screen using a synthetic library of humanized llama single domain antibodies (termed VHH) (Moutel et al., 2016). We have previously shown that peritoneal ascites from patients with cancer contain a population of mo-DC (Segura et al., 2013; Tang-Huau et al., 2018). Cells from tumor ascites were separated into DCs and all other cells (non-DCs), including tumor cells, macrophages, T cells, and other immune cells. The library was first depleted for phages binding to non-DCs, then phages binding to ascites DCs were screened (Figure 1A). For subsequent studies, we produced the VHH of interest with a human Fc region containing a streptavidin-binding peptide. Using this strategy, we identified a VHH antibody, termed "D4," that stains

[1]Institut Curie, PSL Research University, CNRS, UMR144, 26 rue d'Ulm, 75005 Paris, France

[2]Institut Curie, PSL Research University, Centre de Recherche, Laboratoire de Spectrométrie de Masse Protéomique, 26 rue d'Ulm, 75005 Paris, France

[3]Institut Curie, PSL Research University, INSERM, U932, 26 rue d'Ulm, 75005 Paris, France

[4]Lead Contact

*Correspondence: elodie.segura@curie.fr

https://doi.org/10.1016/j.isci.2020.100987

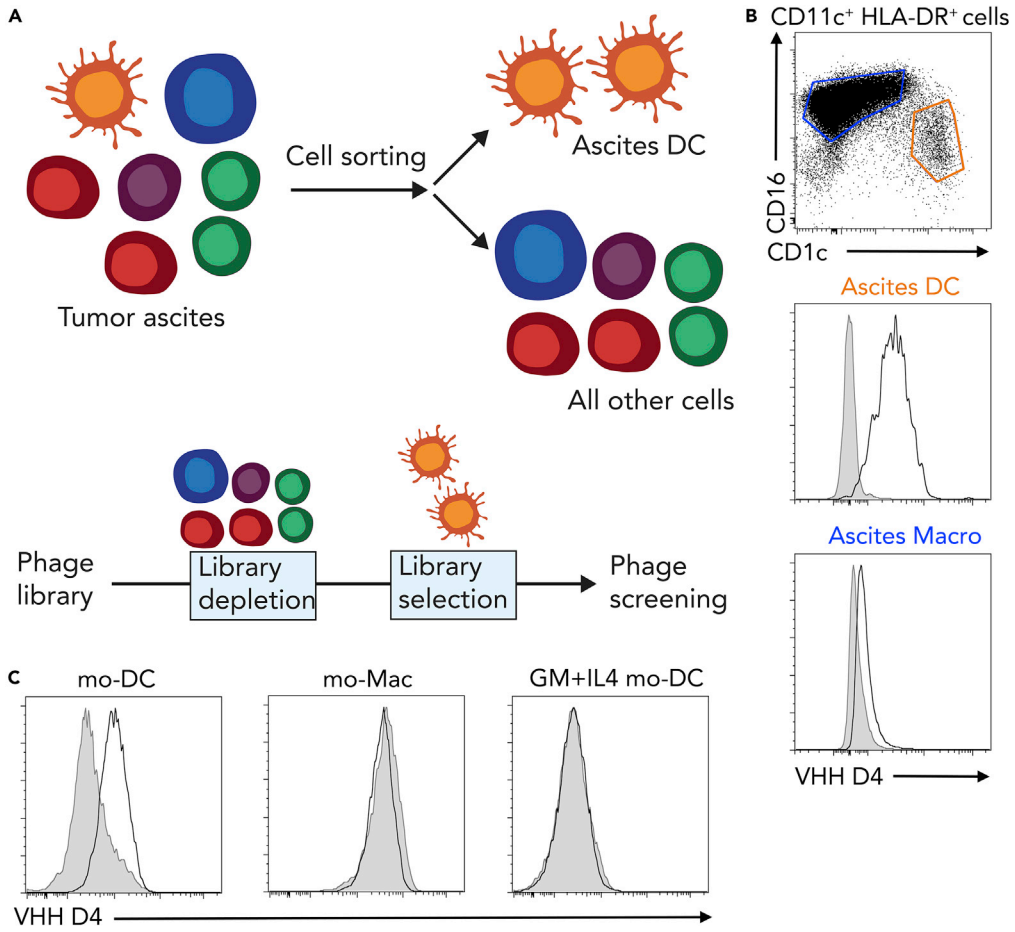

Figure 1. Identification of a VHH Specific for Monocyte-Derived Dendritic Cells

(A) Strategy for identifying novel surface markers for ascites dendritic cells (DCs).

(B) Ascites cells were stained with VHH D4. Stainings for DC and macrophages (Macro) are shown (representative of five individual donors). Gray shaded histograms are fluorescence-minus-one controls.

(C) Monocytes were cultured with M-CSF, IL-4, and TNFa to generate DC (mo-DC) and macrophages (mo-Mac) or with GM-CSF and IL-4 to generate DC (GM + IL4 mo-DC). Cells were stained with VHH D4. Gray shaded histograms are fluorescence-minus-one controls. Representative of four individual donors.

ascites DCs but not macrophages from the same samples (Figure 1B). We have recently reported a culture model allowing the generation of *in vitro* counterparts of naturally occurring mo-DC and mo-Mac, by culturing $CD14^+$ monocytes with M-CSF, IL-4, and TNFα (Goudot et al., 2017). In this model, the VHH D4 stained mo-DC but not mo-Mac (Figure 1C). We have also shown that the classical model of culturing monocytes with GM-CSF and IL-4 generates mo-DC that do not closely resemble the ones found *in vivo* in inflammatory fluids (Goudot et al., 2017). Consistent with this, the VHH D4 did not stain mo-DC generated with GM-CSF and IL-4 (Figure 1C).

We then sought to address whether the VHH D4 could also stain other myeloid cells, in particular cDCs. We first used the VHH D4 on cells isolated from human tonsils. We have previously shown using single-cell RNA sequencing (RNA-seq) analysis that tonsils contain cDC1 ($CD141^{high}CD1c^-$ DCs) and cDC2 ($CD141^{low}CD1c^+$ DCs), but no population of mo-DC (Durand et al., 2019). There was no significant staining of VHH D4 on cDC1, cDC2, or tonsil macrophages (Figure 2A). This result suggests that the VHH D4 is specific of mo-DC and does not stain cDCs.

To extend these observations, we stained peripheral blood cells. There was no significant staining on plasmacytoid DCs (pDC), B cells, granulocytes, NK cells, or T cells (Figure 2B). We further dissected VHH D4

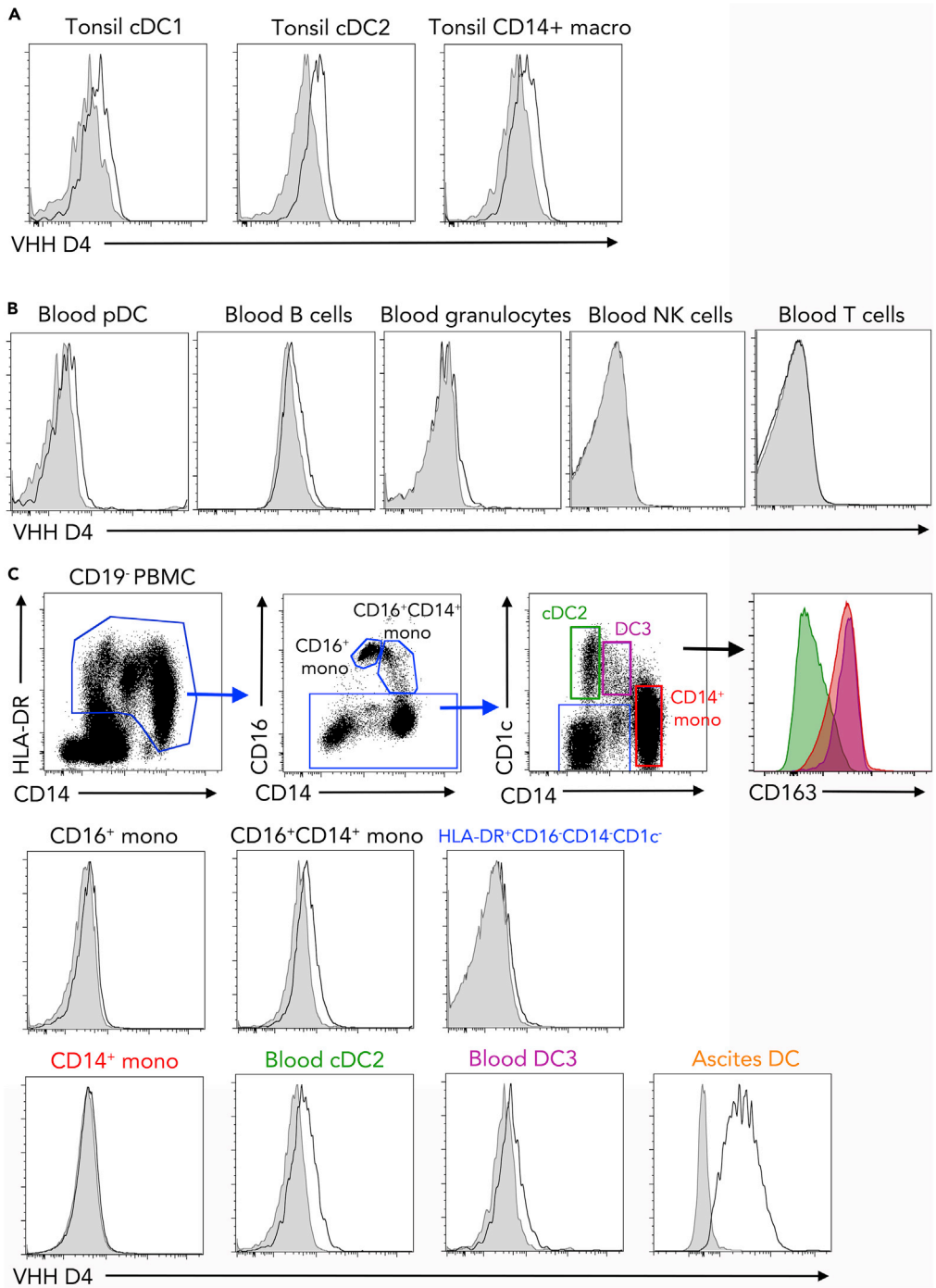

Figure 2. VHH D4 Does Not Stain Classical Dendritic Cell Populations

(A) Tonsil DC and macrophages were stained with VHH D4. Gray shaded histograms are fluorescence-minus-one controls. Representative of two individual donors. Peripheral blood cells (B and C) or ascites cells (C) were stained with VHH D4. Gray shaded histograms are fluorescence-minus-one controls. Representative of five (blood) or four (ascites) individual donors. (C) Gating strategy for analyzing HLA-DR$^+$ cells, including CD14$^+$ monocytes, cDC2, and DC3, is shown. Staining of ascites DC is shown as a positive control.

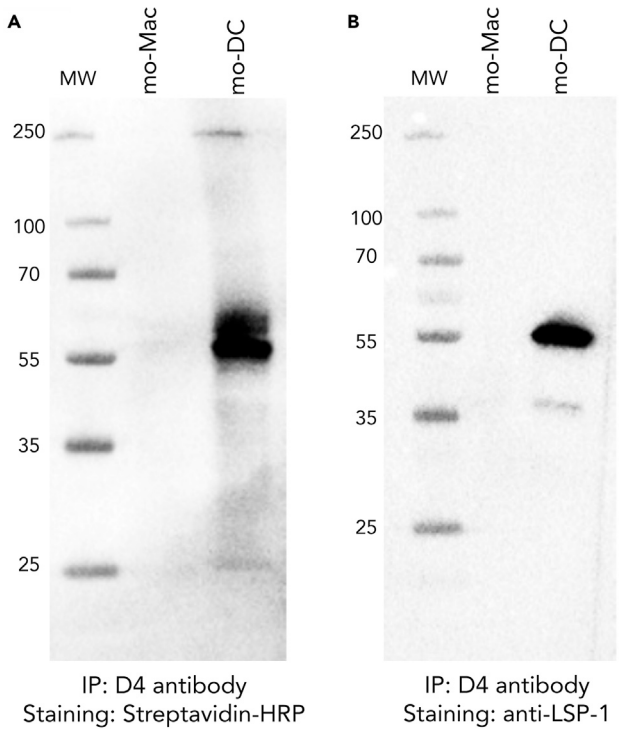

Figure 3. Identification of LSP-1 as the Target of VHH D4

In vitro-generated mo-DC or mo-Mac were incubated with VHH D4, then lysed. Immuno-precipitation was performed on cell lysate using the streptavidin-binding peptide tag. MW, molecular weight. Immuno-precipitated material was analyzed by western blot. Staining was performed using streptavidin-HRP (A) or a commercial anti-LSP-1 antibody (B).

staining on myeloid cells (Figure 2C). Blood monocytes comprise three subpopulations defined by their expression of CD16 and CD14. In addition, it has recently been shown that blood CD1c$^+$ DCs are heterogeneous and comprise CD1c$^+$CD14$^-$CD163$^-$ DCs (*bona fide* cDC2) and CD1c$^+$CD14$^+$CD163$^+$ DCs, termed DC3 (Alcantara-Hernandez et al., 2017; Bakdash et al., 2016; Dutertre et al., 2019; Villani et al., 2017). The VHH D4 did not show a significant staining on blood monocytes, cDC2, DC3, or other CD19$^-$HLA-DR$^+$ cells (Figure 2C). These results confirm that VHH D4 does not recognize cDCs or other blood leukocyte populations.

To determine the target of VHH D4 on the surface of mo-DC, we performed immuno-precipitation followed by proteomics mass spectrometry, using *in vitro*-generated mo-DC (cultured with M-CSF, IL-4, and TNFα) as a source of material. Mass spectrometry identified only one protein: Lymphocyte-Specific Protein 1 (LSP-1), a protein of predicted molecular weight of 60 kDa. To validate this result, we performed immuno-precipitation with VHH D4 on *in vitro*-generated mo-DC and mo-Mac and revealed the immuno-precipitated proteins using streptavidin (Figure 3A) or a commercial anti-LSP-1 antibody (Figure 3B). Both methods showed the same band around 55 kDa, only in immuno-precipitated material from mo-DC. This observation confirms that the VHH D4 binds LSP-1.

LSP-1 is an F-actin binding protein reported to be expressed in all leukocytes (Pulford et al., 1999). Using our previously generated transcriptomic data (Goudot et al., 2017), we confirmed that *LSP1* was expressed at similar levels in ascites mo-DC; ascites macrophages; *in vitro* mo-DC and mo-Mac generated with M-CSF, IL-4, and TNFα; *in vitro* mo-DC generated with GM-CSF and IL-4; and blood monocytes (Figure 4A). Using transcriptomic data from the Human Cell Atlas, we also observed that *LSP1* was expressed in all blood leukocytes, with myeloid cells displaying the highest levels (Figure 4B). To confirm the intracellular expression of LSP-1, we performed flow cytometry on permeabilized cells using either a commercial anti-LSP1 antibody or VHH D4. Although the commercial anti-LSP1 did not show any surface staining (including on mo-DC), it detected intracellular LSP1 in blood myeloid cells and *in vitro*-generated mo-DC and mo-Mac (Figure 4C). By contrast, VHH D4 did not stain intracellular LSP1 in blood myeloid cells or mo-Mac

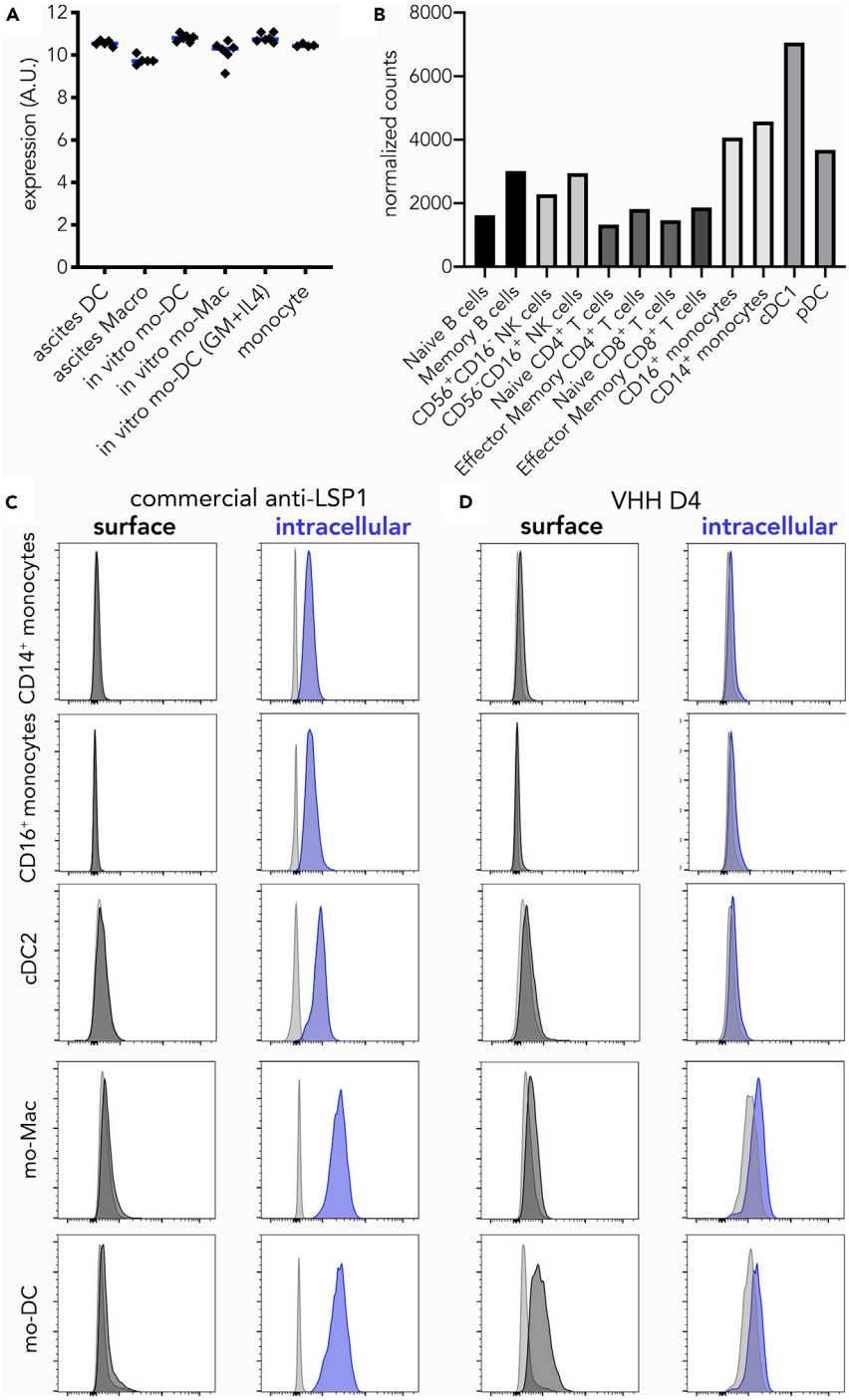

Figure 4. VHH D4 Recognizes a Surface Epitope of LSP-1 Specifically Expressed by mo-DC

(A) Expression levels (arbitrary units) of *LSP1* in ascites DC; ascites macrophages; *in vitro* mo-DC and mo-Mac generated with M-CSF, IL-4, and TNFα; *in vitro* mo-DC generated with GM-CSF and IL-4; and blood $CD14^+$ monocytes. Each dot represents an individual donor. Median is shown. Affymetrix data from dataset GSE102046.

(B) Normalized counts of *LSP1* expression in selected human blood cells. RNA-seq data from the Human Cell Atlas (http://immunecellatlas.net).

(C and D) Monocytes were cultured with M-CSF, IL-4, and TNFα to generate DC (mo-DC) and macrophages (mo-Mac). Peripheral blood myeloid cells were also analyzed (monocytes and cDC2). Cells were stained with a commercial anti-LSP-1 antibody (C) or VHH D4 (D), with membrane permeabilization (intracellular) or not (surface). Gray shaded histograms are fluorescence-minus-one controls. Representative of five (blood) or six (*in vitro*-generated) individual donors.

and mo-DC (Figure 4D). These results suggest that VHH D4 recognizes a surface epitope of LSP-1 that is specifically expressed by mo-DC.

DISCUSSION

Using a synthetic library of humanized llama single domain antibodies, we have identified one antibody, recognizing LSP-1, that is specific for human mo-DC and distinguishes them from monocytes, macrophages, cDCs, or DC3.

LSP-1 has been shown so far to reside on the cytoplasmic side of the plasma membrane (Klein et al., 1989). After membrane permeabilization, LSP-1 can be detected by flow cytometry, consistent with previous work (Pulford et al., 1999). Because VHH D4 stains mo-DC without membrane permeabilization, our results suggest the existence of an extra-cellular domain of LSP-1 specifically in mo-DC. The VHH D4 stains both mo-DC found *in vivo* in tumor ascites and generated *in vitro* with M-CSF, IL-4, and TNFα, indicating that the expression of a surface domain of LSP-1 is not due to the inflammatory micro-environment, but rather could be the result of a mo-DC core transcriptional program. Whether surface LSP-1 results from alternative splicing or another post-transcriptional mechanism remains open for future investigation.

DC3 express a mixed transcriptional program with hallmark cDC2 genes (such as *FCER1A, CD1C, CLEC10A*) as well as typical monocyte genes (such as *S100A8*, *S100A9*, *VCAN*) (Bakdash et al., 2016; Dutertre et al., 2019; Villani et al., 2017), raising the question of their ontogeny, in particular whether DC3 correspond to circulating mo-DC. Our results add to different lines of evidence suggesting that DC3 are distinct from mo-DC. Blood cDC2 and DC3, but not monocytes, were increased upon injection of Flt3-ligand to patients with lymphoma (Dutertre et al., 2019). In addition, *in vitro* differentiation assays and analysis of an allelic series of human IRF8 deficiency suggested that DC3 and monocytes derive from a common progenitor but along distinct differentiation pathways (Cytlak et al., 2019). Here, we did not observe a significant staining of VHH D4 on blood DC3, showing that the phenotype of DC3 is distinct from that of ascites mo-DC. This is consistent with the hypothesis that DC3 do not represent circulating blood mo-DC.

Together with our previous phenotypic characterization of mo-DC (Goudot et al., 2017) and recent single-cell analysis of blood cDC2, DC3, and monocytes (Dutertre et al., 2019; Villani et al., 2017), our work enables a more precise phenotypic definition of human DC subsets. cDC2 can be defined as $CD88^{-}CD14^{-}CD1c^{+}FcεRI^{+}CD226^{-}CD163^{-}sLSP\text{-}1^{-}$, DC3 as $CD88^{-}CD14^{+}CD1c^{+}FcεRI^{+}CD226^{-}CD163^{+}sLSP\text{-}1^{-}$, and mo-DC as $CD88^{low}CD14^{+}CD1c^{+}FcεRI^{+}CD226^{+}CD163^{-}sLSP\text{-}1^{+}$.

Mo-DC have been identified in several inflammatory contexts in human tissues (Coillard and Segura, 2019). In cancer, the picture is less clear as DCs displaying a phenotype consistent with both mo-DC and DC3 have been reported in colorectal, breast, and lung tumors (Laoui et al., 2016; Lavin et al., 2017; Michea et al., 2018). DC3 are increased in the blood of patients with melanoma (Bakdash et al., 2016) and systemic lupus erythematosus (Dutertre et al., 2019), whereas blood DC3 infiltrate the lung alveolar space upon LPS-induced acute inflammation (Jardine et al., 2019). The respective role of these two DC subtypes in cancer or inflammation remains elusive. Our findings will pave the way for a better characterization of DC3 and mo-DC in pathological settings, ultimately allowing their manipulation for therapeutic strategies.

Limitations of the Study

In this work, we have identified one antibody (VHH D4) that is specific for human mo-DC present in ascites or derived *in vitro* from monocytes using a combination of M-CSF, IL-4, and TNFα. Further work is needed to address whether VHH D4 also stains the mo-DC that have been described in other human tissues, such as skin, lung, or gut. In addition, complementary markers, such as defined in the Discussion, should be used for the accurate identification of myeloid cells in human tissues.

METHODS

All methods can be found in the accompanying Transparent Methods supplemental file.

DATA AND CODE AVAILABILITY

Proteomics data are available via ProteomeXchange (identifier PXD015647).

SUPPLEMENTAL INFORMATION

Supplemental Information can be found online at https://doi.org/10.1016/j.isci.2020.100987.

ACKNOWLEDGMENTS

This work was supported by Inserm, CNRS, Agence Nationale de la Recherche (ANR-10-LABX-0043, ANR-CHIN-0002, ANR-10-IDEX-0001-02 PSL), Institut Curie (CIC IGR-Curie 1428), the European Research Council (2013-AdG N° 340046 DCBIOX), and Cancéropôle Île-de-France (2017-1-EMERG-56-ICR-1).

The authors wish to thank A. Coillard for technical assistance, the Flow Cytometry Platform of Institut Curie for cell sorting and the TAb-IP platform of Institut Curie for the production of the VHH.

AUTHOR CONTRIBUTIONS

S.M., S.A., F.P., and E.S. designed experiments. S.M., A.B., A.S., B.L., and E.S. performed experiments. S.M., A.B., D.L., and E.S. analyzed the data. E.S. prepared the figures and wrote the manuscript, with input from all authors.

DECLARATION OF INTERESTS

S.M., S.A., F.P., and E.S. are co-inventors of a patent entitled "New anti-LSP1 antibody" (PCT/EP2017/0761). S.M. and F.P. are co-inventors of a patent that covers the commercial use of the library (WO/2015/063331). The authors declare no other competing interest. The authors adhere to Cell Press policy on sharing materials.

Received: October 5, 2019
Revised: February 21, 2020
Accepted: March 11, 2020
Published: April 24, 2020

REFERENCES

Alcantara-Hernandez, M., Leylek, R., Wagar, L.E., Engleman, E.G., Keler, T., Marinkovich, M.P., Davis, M.M., Nolan, G.P., and Idoyaga, J. (2017). High-dimensional phenotypic mapping of human dendritic cells reveals interindividual variation and tissue specialization. Immunity *47*, 1037–1050.e6.

Bakdash, G., Buschow, S.I., Gorris, M.A., Halilovic, A., Hato, S.V., Skold, A.E., Schreibelt, G., Sittig, S.P., Torensma, R., Duiveman-De Boer, T., et al. (2016). Expansion of A Bdca1+Cd14+ myeloid cell population in melanoma patients may attenuate the efficacy of dendritic cell vaccines. Cancer Res. *76*, 4332–4346.

Coillard, A., and Segura, E. (2019). In vivo differentiation of human monocytes. Front. Immunol. *10*, 1907.

Cytlak, U., Resteu, A., Pagan, S., Green, K., Milne, P., Maisuria, S., Mcdonald, D., Hulme, G., Filby, A., Carpenter, B., et al. (2019). Differential Irf8 Requirement Defines Two Pathways of Dendritic Cell Development in Humans (SSRN).

Durand, M., Walter, T., Pirnay, T., Naessens, T., Gueguen, P., Goudot, C., Lameiras, S., Chang, Q., Talaei, N., Ornatsky, O., et al. (2019). Human lymphoid organ Cdc2 and macrophages play complementary roles in T follicular helper responses. J. Exp. Med. *216*, 1561–1581.

Dutertre, C.A., Becht, E., Irac, S.E., Khalilnezhad, A., Narang, V., Khalilnezhad, S., Ng, P.Y., Van Den Hoogen, L.L., Leong, J.Y., Lee, B., et al. (2019). Single-cell analysis of human mononuclear phagocytes reveals subset-defining markers and identifies circulating inflammatory dendritic cells. Immunity *51*, 573–589.e8.

Ginhoux, F., and Guilliams, M. (2016). Tissue-resident macrophage ontogeny and homeostasis. Immunity *44*, 439–449.

Goudot, C., Coillard, A., Villani, A.C., Gueguen, P., Cros, A., Sarkizova, S., Tang-Huau, T.L., Bohec, M., Baulande, S., Hacohen, N., et al. (2017). Aryl hydrocarbon receptor controls monocyte differentiation into dendritic cells versus macrophages. Immunity *47*, 582–596 E6.

Guilliams, M., Ginhoux, F., Jakubzick, C., Naik, S.H., Onai, N., Schraml, B.U., Segura, E., Tussiwand, R., and Yona, S. (2014). Dendritic cells, monocytes and macrophages: a unified nomenclature based on ontogeny. Nat. Rev. Immunol. *14*, 571–578.

Jakubzick, C.V., Randolph, G.J., and Henson, P.M. (2017). Monocyte differentiation and antigen-presenting functions. Nat. Rev. Immunol. *17*, 349–362.

Jardine, L., Wiscombe, S., Reynolds, G., Mcdonald, D., Fuller, A., Green, K., Filby, A., Forrest, I., Ruchaud-Sparagano, M.H., Scott, J., et al. (2019). Lipopolysaccharide inhalation recruits monocytes and dendritic cell subsets to the alveolar airspace. Nat. Commun. *10*, 1999.

Klein, D.P., Jongstra-Bilen, J., Ogryzlo, K., Chong, R., and Jongstra, J. (1989). Lymphocyte-specific Ca2+-binding protein Lsp1 is associated with the cytoplasmic face of the plasma membrane. Mol. Cell Biol *9*, 3043–3048.

Laoui, D., Keirsse, J., Morias, Y., Van Overmeire, E., Geeraerts, X., Elkrim, Y., Kiss, M., Bolli, E., Lahmar, Q., Sichien, D., et al. (2016). The tumour microenvironment harbours ontogenically distinct dendritic cell populations with opposing effects on tumour immunity. Nat. Commun. *7*, 13720.

Lavin, Y., Kobayashi, S., Leader, A., Amir, E.D., Elefant, N., Bigenwald, C., Remark, R., Sweeney, R., Becker, C.D., Levine, J.H., et al. (2017). Innate immune landscape in early lung adenocarcinoma by paired single-cell analyses. Cell *169*, 750–765.e17.

Michea, P., Noel, F., Zakine, E., Czerwinska, U., Sirven, P., Abouzid, O., Goudot, C., Scholer-Dahirel, A., Vincent-Salomon, A., Reyal, F., et al. (2018). Adjustment of dendritic cells to the

breast-cancer microenvironment is subset specific. Nat. Immunol. *19*, 885–897.

Moutel, S., Bery, N., Bernard, V., Keller, L., Lemesre, E., De Marco, A., Ligat, L., Rain, J.C., Favre, G., Olichon, A., and Perez, F. (2016). NaliH1: a universal synthetic library of humanized nanobodies providing highly functional antibodies and intrabodies. Elife *5*, e16228.

Pulford, K., Jones, M., Banham, A.H., Haralambieva, E., and Mason, D.Y. (1999). Lymphocyte-specific protein 1: a specific marker of human leucocytes. Immunology *96*, 262–271.

Segura, E., Touzot, M., Bohineust, A., Cappuccio, A., Chiocchia, G., Hosmalin, A., Dalod, M., Soumelis, V., and Amigorena, S. (2013). Human inflammatory dendritic cells induce Th17 Cell differentiation. Immunity *38*, 336–348.

Tang-Huau, T.L., Gueguen, P., Goudot, C., Durand, M., Bohec, M., Baulande, S., Pasquier, B., Amigorena, S., and Segura, E. (2018). Human in vivo-generated monocyte-derived dendritic cells and macrophages cross-present antigens through a vacuolar pathway. Nat. Commun. *9*, 2570.

Villani, A.C., Satija, R., Reynolds, G., Sarkizova, S., Shekhar, K., Fletcher, J., Griesbeck, M., Butler, A., Zheng, S., Lazo, S., et al. (2017). Single-cell RNA-Seq reveals new types of human blood dendritic cells, monocytes, and progenitors. Science *356*, eaah4573.

iScience, Volume *23*

Supplemental Information

Surface LSP-1 Is a Phenotypic Marker Distinguishing Human Classical versus Monocyte-Derived Dendritic Cells

Sandrine Moutel, Anne Beugnet, Aurélie Schneider, Bérangère Lombard, Damarys Loew, Sebastian Amigorena, Franck Perez, and Elodie Segura

Supplemental Information

Transparent methods

Human Samples. Buffy coats from healthy donors (both male and female donors) were obtained from Etablissement Français du Sang (Paris, France) in accordance with INSERM ethical guidelines. Tumor ascites from ovarian cancer patients were obtained from Hôpital de l'Institut Curie in accordance with hospital guidelines. Tonsils from healthy patients (both male and female) undergoing tonsillectomy were obtained from Hôpital Necker (Paris, France). According to French Public Health Law (article L1121), written consent and IRB approval are not required for human non-interventional studies.

Cell isolation. Tonsil samples were digested as described previously (Durand and Segura, 2016). In brief, samples were cut into small fragments, digested with 0.1 mg mL^{-1} Liberase TL (Roche) in the presence of 0.1 mg mL^{-1} DNAse (Roche) for 40 minutes at room temperature before addition of 10 mM EDTA. Cells were filtered on a 40 μm cell strainer (BD Falcon) and washed. Light density cells were isolated by centrifugation on a Ficoll gradient (Lymphoprep, Greiner Bio-One). DCs and macrophages were enriched by depletion of cells expressing CD3, CD15, CD19, CD56 and CD235a using antibody-coated magnetic beads (Miltenyi). Peripheral Blood Mononuclear Cells (PBMC) were prepared by centrifugation on a Ficoll gradient. Blood $CD14^+$ monocytes were isolated from healthy donors' PBMC by positive selection using anti-CD14-coated magnetic beads according to manufacturer's instructions (Miltenyi). DCs and macrophage populations from ascites were isolated after cell sorting on a FACSAria instrument. Ascites DCs were gated as HLA-$DR^+CD11c^+CD1c^+CD16^-$.

Cell culture. Blood monocytes (1×10^6 cells mL^{-1}) were cultured for 5 days in RPMI-Glutamax medium (Gibco) supplemented with antibiotics (penicillin and streptomicin) and 10% FCS in the presence of 100 ng mL^{-1} M-CSF (Miltenyi), 5 ng mL^{-1} IL-4 (Miltenyi) and 5 ng mL^{-1} TNF-

α (Miltenyi), or 100 ng mL^{-1} GM-CSF (Miltenyi) and 5 ng mL^{-1} IL-4 (Miltenyi). In some experiments, mo-DC and mo-Mac were purified by cell sorting on a FACSAria instrument. Mo-DC were gated as $CD1a^{+}CD16^{-}$ and mo-mac as $CD1a^{-}CD16^{+}$.

Phage display screening. A synthetic phage display library of humanized llama single domain antibodies (NaLi-H1 library) was used as described (Moutel et al., 2016) to select binders. Screening of positive clones was performed using 100 µL of supernatant (80 µL phages + 20 µL PBS/human serum 1%) incubated for 1 h on ice with 1×10^{5} cells from tumor ascites. After washing, phage binding on ascites cells was detected by flow cytometry using an antibody against M13, and ascites DCs were gated as $HLA\text{-}DR^{+}CD11c^{+}CD1c^{+}CD16^{-}$ and ascites macrophages as $HLA\text{-}DR^{+}CD11c^{+}CD1c^{-}CD16^{+}$.

Western blot. Cells were lysed in RIPA buffer (Thermo Scientific) supplemented with cOmplete Mini EDTA-free protease inhibitor cocktail (Roche). Post-nuclear lysates were resolved by SDS-PAGE using 4-12% BisTris NuPAGE gels (Invitrogen) and proteins were transferred to membranes (Immunoblot PVDF membranes, Bio-Rad). Membranes were stained with anti-LSP1 (clone TPD153, Novus Biologicals) or streptavidin-HRP staining (Pierce).

Flow cytometry. For the analysis of tonsil cells, tonsil $CD14^{+}$ macrophages were gated as $HLA\text{-}DR^{+}CD11c^{+}CD14^{+}$, tonsil cDC1 as $HLA\text{-}DR^{+}CD11c^{+}CD14^{-}CD1c^{-}CD141^{+}$ and tonsil cDC2 as $HLA\text{-}DR^{+}CD11c^{+}CD14^{-}CD1c^{+}$. For the analysis of blood cells, B cells were gated as $HLA\text{-}DR^{+}CD19^{+}$, pDC as $HLA\text{-}DR^{+}CD19^{-}CD11c^{-}CD123^{+}$, granulocytes as $HLA\text{-}DR^{-}CD19^{-}SSC^{high}CD16^{+}$, NK cells as $HLA\text{-}DR^{-}CD19^{-}CD14^{-}SSC^{low}CD16^{+}$, T cells as $HLA\text{-}DR^{-}CD19^{-}CD14^{-}SSC^{low}CD16^{-}$, $CD16^{+}$ monocytes as $HLA\text{-}DR^{+}CD19^{-}CD16^{+}CD14^{-}$, $CD16^{+}CD14^{+}$ monocytes as $HLA\text{-}DR^{+}CD19^{-}CD16^{+}CD14^{+}$, $CD14^{+}$ monocytes as $HLA\text{-}DR^{+}CD19^{-}CD16^{-}CD14^{+}CD1c^{-}$, cDC2 as $HLA\text{-}DR^{+}CD19^{-}CD16^{-}CD14^{-}CD1c^{+}$, DC3 as $HLA\text{-}DR^{+}CD19^{-}CD16^{-}CD14^{int}CD1c^{+}$.

Flow cytometry stainings were performed at 4°C in PBS containing 2mM EDTA (Gibco) and 0.5% human serum AB male (Biowest). Antibodies used were : FITC anti-CD19 (clone HIB19, BioLegend), FITC anti-CD3 (clone UCHT1, BioLegend), FITC anti-CD16 (clone 3G8, Biolegend), PE anti-M13 (GE healthcare), PE anti-CD19 (clone SJ25C1, eBioscience), PE anti-CD141 (clone AD5-14H12, Miltenyi biotec), Pe/Cy7 anti-CD11c (clone Bu15, Biolegend), Pe/Cy7 anti-CD163 (clone GHI/61, eBioscience), PerCP-eFluor710 anti-CD1c (clone L161, eBioscience), APC anti-CD304 (clone REA774, Miltenyi biotec), APC anti-CD1a (clone HI149, BioLegend), Alexa647 anti-LSP1 (clone TPD153, Novus Biologicals), APC-eFluor780 anti-HLA-DR (clone LN3e, Bioscience), HorizonV500 anti-CD14 (cloneM5E2, BD). In some experiments, cells were stained with Streptavidin-PE (BD), Streptavidin-APC (BD) or Streptavidin-PeCy7 (BD). Fc receptor binding was blocked using TruStain FcX (BioLegend). Dead cells were excluded with 4′,6-diamidino-2-phenylindole (DAPI, Thermo Fisher) staining. For intracellular staining, cells were first surface stained as above, then incubated with Live/dead fixable Aqua (Thermo Fisher Scientific) for 10 min at 4°C. Then the cells were fixed and permeabilized using Intracellular Fixation & Permeabilization Buffer Set (eBioscience). Unspecific binding was blocked by incubating cells for 30 min at 4°C with blocking buffer (Perm/Wash buffer from Intracellular Fixation & Permeabilization Buffer Set containing 2% of normal mouse serum and 10µg/mL human Fc block (BD)). Cells were stained for intracellular molecules in blocking buffer at room temperature for 30 min. For VHH D4 intracellular staining, cells were further incubated with Streptavidin-APC (BD) for 15 min at 4°C in blocking buffer. Cells were analyzed on a FACSVerse or LSRII (BD Biosciences) instrument. Data was analyzed with FlowJo (Tree Star).

Immuno-precipitation. All the incubation steps were performed rocking the tubes constantly. Cleared cell lysates resuspended in an equal volume of IP buffer (10 mM Tris–HCl, pH 8.0, 150 mM NaCl, 1% NP40) were pre-incubated 1 h at 4°C in the presence of 200 µL of protein

G agarose beads (Thermo Fisher) and successively washed 3 times in IP buffer to eliminate unspecific binding. The supernatant was recovered by centrifugation (3 min × 2500 g), mixed with 200 µg of antibody, and incubated 2 h at 4°C. Finally, 200 µL of washed protein G agarose beads were added and washed after 1 h at 4°C 5 times in 10 mL of IP buffer five times before being resuspended in 50 µL of SDS loading buffer and heated 10 min at 95°C.

Proteomics Mass-spectrometry. Immuno-precipitation was performed with VHH D4 on *in vitro*-generated mo-DC. Two bands were obtained for the immuno-precipitated material after SDS-PAGE migration (molecular weight around 60 kDa and 45-50 kDa respectively). Gel slices were washed and proteins were reduced with 10 mM DTT before alkylation with 55 mM iodoacetamide. After washing and shrinking the gel pieces with 100% (vol/vol) MeCN, we performed in-gel digestion using trypsin (Roche) overnight in 25 mM NH_4HCO_3 at 30 °C. Peptides extracted from each band were analyzed by nanoLC-MS/MS using an Ultimate 3000 system (Dionex, Thermo Scientific, Waltham, MA) coupled to a TripleTOF™ 6600 mass spectrometer (ABSciex). For identification, data was searched against the Swissprot fasta database containing *Homo Sapiens* (2014_10, 20194 sequences) using Mascot™ (version 2.3.02) and further analyzed in myProMS (Poullet et al., 2007). The maximum false discovery rate (FDR) calculation was set to 1% at the peptide level for the whole study (QVALITY algorithm). Only proteins found in two experiments and not in the control IPs were considered candidates. Only one candidate was identified (P33241, Lymphocyte-specific protein 1), with scores of 403.47 and 499.61, and coverage of 23.9% and 26.3%, for the two bands, respectively. Data is available via ProteomeXchange (identifier PXD015647) (Vizcaino et al., 2016).

Supplemental References

Durand, M. & Segura, E. 2016. Dendritic Cell Subset Purification From Human Tonsils And Lymph Nodes. *Methods Mol Biol,* 1423**,** 89-99.

Moutel, S., Bery, N., Bernard, V., Keller, L., Lemesre, E., De Marco, A., Ligat, L., Rain, J. C., Favre, G., Olichon, A. & Perez, F. 2016. Nali-H1: A Universal Synthetic Library Of Humanized Nanobodies Providing Highly Functional Antibodies And Intrabodies. *Elife,* 5.

Poullet, P., Carpentier, S. & Barillot, E. 2007. Myproms, A Web Server For Management And Validation Of Mass Spectrometry-Based Proteomic Data. *Proteomics,* 7**,** 2553-6.

Vizcaino, J. A., Csordas, A., Del-Toro, N., Dianes, J. A., Griss, J., Lavidas, I., Mayer, G., Perez-Riverol, Y., Reisinger, F., Ternent, T., Xu, Q. W., Wang, R. & Hermjakob, H. 2016. 2016 Update Of The Pride Database And Its Related Tools. *Nucleic Acids Res,* 44**,** 11033.